Journal Pre-proofs

Ag/Ag_2O confined visible-light driven catalyst for highly efficient selective hydrogenation of nitroarenes inpure watermedium at room temperature

Zhengliang Yin, Liangxu Xie, Shunsheng Cao, Yingguan Xiao, Gang Chen, Ying Jiang, Wenxian Wei, Limin Wu

PII: S1385-8947(20)31028-7
DOI: https://doi.org/10.1016/j.cej.2020.125036
Reference: CEJ 125036

To appear in: *Chemical Engineering Journal*

Received Date: 11 February 2020
Revised Date: 4 April 2020
Accepted Date: 7 April 2020

Please cite this article as: Z. Yin, L. Xie, S. Cao, Y. Xiao, G. Chen, Y. Jiang, W. Wei, L. Wu, Ag/Ag_2O confined visible-light driven catalyst for highly efficient selective hydrogenation of nitroarenes inpure watermedium at room temperature, *Chemical Engineering Journal* (2020), doi: https://doi.org/10.1016/j.cej.2020.125036

Chemical Engineering Journal, Volume 394, 15 August 2020, Article number 125036
DOI:10.1016/j.cej.2020.125036

Ag/Ag_2O confined visible-light driven catalyst for highly efficient selective hydrogenation of nitroarenes in pure water medium at room temperature

Zhengliang Yin,[a] Liangxu Xie,[c] Shunsheng Cao, [a,d]* Yingguan Xiao, [a] Gang Chen, [a] Ying Jiang, [d] Wenxian Wei, [e] and Limin Wu [b*]

[a] *Research School of Polymer Materials, School of Materials Science & Engineering, Jiangsu University, Zhenjiang 212013, China.*

[b] *Department of Materials Science and State Key Laboratory of Molecular Engineering of Polymers, Fudan University, Shanghai, 200433, China.*

[c] *Institute of Bioinformatics and Medical Engineering, School of Electrical and Information Engineering, Jiangsu University of Technology, Changzhou, 213001, China.*

[d] *School of Water, Energy and Environment, Cranfield University, Bedford MK43 0AL, UK.*

[e] *Testing Center, Yangzhou University, Yangzhou, Jiangsu 225009, China*

[*] Corresponding Author * E-mail: sscao@ujs.edu.cn; lmw@fudan.edu.cn

Abstract: Although photocatalysis has attracted tremendous research interest, there still remains critical challenges (*e.g.,* low visible-light quantum efficiency, organic media, *etc.*), especially for selective hydrogenation of nitroarenes. Herein, we design and synthesize the first confined photocatalyst by introducing the nanospace of double-shelled hollow silica sphere as a photocatalytic nanoreactor to promote the hydrogenation reaction with the fast reaction kinetics. This photocatalyst exhibits excellent activity, selectivity, and recyclability. Especially, superior selectivity (>99%) is achieved when used for the hydrogenation of nitroarenes under visible-light irradiation in pure water medium. Both experimental and theoretical simulation results indicate that the Ag/Ag_2O structure and confined nanospace of the photocatalyst greatly increase the contact probability between photogenerated atomic hydrogen and nitroarenes. Additionally, corresponding anilines are obtained almost quantitatively towards the hydrogenation of nitroarenes in pure water medium at room temperature. Therefore, this work provides a rational design concept of highly efficient visible-light photocatalyst for green chemistry industry.

Keywords: Photocatalytic nanoreactor; Nitroarenes; Confinement effect; Visible-light irradiation; Superior selectivity

1. Introduction

Exploring highly efficient catalysts for the hydrogenation of nitroarenes to anilines is of significance because the functionalized anilines and their derivatives are key chemical intermediates for the manufacture of pharmaceutical, agrochemical, and pigment industries [1-3]. Compared with metal nanoparticle (MNP) catalysts, the supported MNPs catalysts can avoid the MNPs aggregation and offer improved performance in catalytic reduction of various nitroaromatics [4-6]. Especially, the development of highly selective, earth-abundant, atom-efficient and recyclable catalysts has been attracting much interest in order to meet the substantially industrial requirements owing to the high-cost and limited availability of noble metals [3,4,7]. Transitional metals, alloy or single-atom catalysts have shown some promise as alternative solutions to increase the activity and selectivity towards the hydrogenation of nitroarenes in recent years [7-10]. However, there still remain some drawbacks including long reaction time, high temperature, and pressured hydrogen gas for these supported metal catalysts [6,11-13]. And due to the stepwise reduction of nitroarenes during the hydrogenation processes, a lot of by-products such as nitroso- and azo-compounds are produced, severely limiting the practical applications of these catalysts in industry [3,6,14].

Using solar energy to directly drive the hydrogenation of nitroarenes into anilines can avoid the formation of byproducts and exhibit a high reaction rate and selectivity under benign reaction conditions without high-pressure hydrogen gas [14-16]. Currently, various semiconductors including SiC [15], Si [17], and g-C_3N_4 [18] have been reported as effective catalysts for the light-driven hydrogenation of nitroarenes. For example, Au-Cu@ZrO_2 photocatalyst was reported to yield the corresponding

anilines directly as the sole product under visible-light irradiation [14]. MNPs loaded Si catalyst was effective towards the photoinduced hydrogenation of nitrobenzene to corresponding aniline under light irradiation [17]. However, the quantum efficiencies reported in these studies are quite low under visible-light irradiation at ambient temperature, even using supported noble metal photocatalysts [3,19]. This issue is especially critical for realizing highly efficient light-driven organic synthesis when hydrogen transfer steps from hydrogen donor to organic substrates are involved in the hydrogenation reaction [3], [16]. Not only that, all these conventional supported metal catalysts have to rely on organic solvents as reaction media to promote the diffusion rate of substrate due to the low water solubility of nitroarenes (*e.g.*, nitrobenzene, chloronitrobenzene, *etc*.) [14,15,17,20-24]. Although a couple of works tried to use aqueous systems to hydrogenate nitroarenes, their atomic hydrogen was produced mainly based on the reaction between metal [18] or $NaBH_4$ [25] with water rather than photoinduced atomic hydrogen, leading to a relatively low conversion [18, 25, 26], as a result, high reaction temperature combined with long reaction time were used to boost the photocatalytic process [26]. Therefore, how to enhance the diffusion- and hydrogen transfer- independent photocatalytic reaction remains a big challenge for the hydrogenation of nitroarenes in pure water medium at room temperature.

Herein, we report a novel visible-light driven photocatalyst by introducing the nanospace of double-shelled hollow silica spheres as a photocatalytic nanoreactor for the first time, in which the confined Ag/Ag_2O nanoparticles (metal-semiconductor) are easy to be excited and generate lots of electron/hole pairs under visible-light irradiation for quick hydrogenation reaction even in pure aqueous media because photoinduced atomic hydrogen can rapidly be transferred to nitroarenes in the confined nanospace [14,15,17,18,20-24,26]. Although confined concept has been widely used for designing common catalysts, it has never been

used for light-driven catalysts owing to the optical opacity of supports (Figure S1). Both the experimental results and molecular dynamics (MD) simulation illustrate that the special confined environment can significantly boost the contact probability between nitroarene molecules and photogenerated atomic hydrogen, which is too difficult to be realized in currently all photocatalytic systems. Accordingly, the obtained novel photocatalyst presents extremely high activity, selectivity, and stability even in pure water medium at room temperature, significantly promoting the green synthesis of key chemical intermediates in industry. Our findings provide a design idea to develop novel highly efficient, low-cost and environment-friendly photocatalysts.

2. Experimental Section

1.1 Materials and methods

Tetraethoxysilane (TEOS), 2-(methacryloyloxy) ethyltrimethylammonium-chloride (DMC), and allyl triethoxysilane (ATES) were obtained from J&K scientific Ltd and used as received without further purification. Silver nitrate, sodium borohydride, styrene, $K_2S_2O_8$, and 2-propanol were available from the Sinopharm Chemical Reagent Co., LtdS (China) and were used as received except styrene was purified with 5 wt.% sodium hydroxide before use.

1.2 Silver ions encapsulation

hollow SiO_2 spheres were synthesized according to our previous works [27,28]. Subsequently, silver nitrate was added to aqueous solution using hollow SiO_2 as template *via* the impregnation method [29]. Typically, hollow SiO_2 spheres (4 g) were added to 40 mL of aqueous solution containing the required amount of silver nitrate. The mixture was stirred for 24 h, evaporated and dried under vacuum overnight.

1.3 Preparation of SiO_2-Ag/Ag_2O/void@SiO_2 photocatalyst

The as-synthesized hollow SiO_2-Ag^+ spheres (0.4 g) were used as the template and *in situ* polymerized with styrene (2.5 g) and co-monomer DMC (0.6 g), and further coated by silica shell derived from the sol-gel reaction of TEOS (1.5 g) under the ammonia (3 mL). After calcination at 450℃, the resulting particles were reduced to Ag, Ag/Ag_2O, and Ag_2O nanoparticles using an excess amount of $NaBH_4$, small amount of $NaBH_4$ and without $NaBH_4$, producing SiO_2-Ag/void@SiO_2, SiO_2-Ag/Ag_2O/void@SiO_2, and SiO_2-Ag_2O/void@SiO_2, responsively. For comparison, the SiO_2-Ag/Ag_2O@SiO_2 (without confined nanospace) and SiO_2/void@SiO_2-Ag/Ag_2O (unconfined catalyst) were also synthesized using the same synthetic process of SiO_2-Ag/Ag_2O/void@SiO_2 photocatalyst.

1.4 Photocatalytic hydrogenation of nitroarenes

Photocatalyst (25 mg) was added to a H_2O/2-propanol (10.2 mL) at the ratio of 9:1 w/w (10:90) or pure water (10.2 mL). After degased by bubbling nitrogen, nitroarenes (0.05 mmol) and formic acid (8.3 mg) were added. The sealed test tube was positioned in a quartz bath and the suspension was stirred and illuminated by visible-light irradiation (Perfectlight, PLS-SXE300, xenon lamp with an UV cut-off filter (λ>400 nm)). As soon as the catalyst was added, the hydrogenation products of nitroarenes were detected by high performance liquid chromatography (HPLC).

3. Results and Discussion

3.1 The preparation and characterization of the confined SiO_2-Ag/Ag_2O/void@SiO_2 photocatalyst

The visible-light driven catalyst is prepared as illustrated in Figure 1a. the silver ions (Ag^+) are deposited on the surface of hollow silica spheres to form SiO_2-Ag^+ nanoparticles, which are then encapsulated by cationic polystyrene spheres (CPS)

through the copolymerization of styrene and allyltrimethoxysilane monomer [27]. During this process, the outer SiO_2 shell is formed *via* the sol-gel reaction of tetraethyl orthosilicate (TEOS). After removing templates via calcination at 450°C, followed by the partial reduction using a catalytic amount of $NaBH_4$, SiO_2-Ag/Ag_2O/void@SiO_2 photocatalyst is obtained.

The TEM image shows a sharp difference between the pale hollow center and the dark solid edge (Figure 1b), indicating that each sphere has a hollow structure. A closer observation finds a clear double ring at the surfaces of all spheres, indicating a double-shelled hollow SiO_2 structure. This structure can be further confirmed by the SEM image (Figure 1c) showing a well-defined morphology and artificially broken microspheres (insert). In addition, the high-resolution TEM (HRTEM) reveals that each hybrid sphere contains a number of dark particles with crystal lattices of 0.204 nm and 0.270 nm (Figure 1d), which correspond to Ag and Ag_2O, respectively [30] and confirm the successful formation of both Ag and Ag_2O nanoparticles through partial reduction using $NaBH_4$.

X-ray diffraction (XRD) analysis also reveals diffraction peaks at 32.2°, 38.0°, 54.8°, and 64.3°, and at 38.1°, 44.3°, 64.4°, and 77.4° (Figure. S2a), corresponding to Ag_2O (JCPDS No. 41-1104) and metallic Ag (JCPDS No. 04-0783) [30], respectively. The content of Ag/Ag_2O mixture in the as-obtained hybrid sphere is ~53.2 mg/g measured by inductively coupled plasma-optical emission spectroscopy (ICP-OES). N_2 adsorption/desorption isotherm displays a type IV with a distinct hysteresis loop observed in the almost whole range (0.05–0.9 P/P_0) (Figure 1e), which is distinguished from the same condensation steps of single-shelled hollow silica [31]. Moreover, the BET (Brunauer-Emmet-Teller) isotherms and BJH (Barrett-Joyner-Halenda) pore size distributions indicate that the hybrid sphere has mesoporous structure with a high

surface area of 141.68 m^2/g, making it more convenient for reactants/products to diffuse to/from the confined Ag/Ag_2O sites. The energy dispersive X-ray (EDX) analysis shows the presence of C, O, Si, and Ag elements (Figure S2b). The elemental mapping further demonstrates that Si and O signals hold the same morphology of double-shelled hollow silica sphere (Figure 1f-h). Moreover, the Ag element is highly distributed in sample (Figure. 1i). The elemental profiles also show that silver signal appears after the signals of silicon and oxygen, then the strong signals of silicon and oxygen elements again (Figure S3). Combined with Figure. 1, the Ag/Ag_2O confined in the double-shell hollow silica spheres have been successfully prepared [32].

3.2 Bonding environment of SiO_2-Ag/Ag_2O/void@SiO_2 photocatalyst

The full survey XPS spectrum shows the existences of O, Ag, C, and Si in the form of O1s, Ag3d, C1s, and Si2s (Figure S4a). For the Ag_2O nanoparticles, the spin-orbit components of Ag3d peak are located at ~374.55 and 368.3 eV (Figure S4b), which correspond to Ag^+ in crystal structure of Ag_2O [33]. Interestingly, the two strong peaks are able to been divided into four bands (367.7, 368.8, 373.7 and 374.8 eV), indicating the existence of multiple valences of silver species. The two relatively weak peaks at 368.8 and 374.8 eV are indexed to $Ag^{\circ}3d_{5/2}$ and $3d_{3/2}$, respectively, while the two major peaks at about 367.7 and 373.7 eV are assigned to $Ag3d_{5/2}$ and $Ag3d_{3/2}$, indicating that Ag element mainly exists as Ag_2O. The high-resolution O1s spectrum may be attributed to the O element in hollow SiO_2 sample (Figure S4c), and can be fitted into four peaks, in which Ag-O characteristic peak appears at 529.4 eV [33], while other peaks of O1s can be ascribed to the oxygen in the surface hydroxyl groups as well as carbonate species [34]. Consequently, all these results confirm that the Ag/Ag_2O confined in the nanospace of double-shelled hollow SiO_2 spheres have been successfully synthesized.

3.3 Photocatalytic hydrogenation of nitroarenes

Hydrogenation of nitroarenes is an important industrial reaction to produce high-value-added amines, and usually used as a model reaction to prove the photocatalytic properties of the as-synthesized catalysts [1,35,36]. Herein, two controls, one is the Ag nanoparticles confined in double-shelled hollow SiO_2 spheres (SiO_2-Ag/void@SiO_2) and another is the Ag_2O nanoparticles confined in double-shelled hollow SiO_2 spheres (SiO_2-Ag_2O/void@SiO_2), were synthesized for further comparison to understand the respective role of Ag and Ag_2O species by using the photocatalytic hydrogenation of nitroarenes to produce aniline under visible-light irradiation (λ>400 nm) and formic acid as a hydrogen source, which was widely reported as the transfer hydrogenation of nitroarenes [8,37]. As shown in Table.1, when the hydrogenation reaction takes place in an organic solvent, *e.g.*, 2-propanol with H_2O (9:1 w/w), SiO_2-Ag/void@SiO_2 presents the poorest conversion and selectivity towards the hydrogenation of three nitroarenes (nitrobenzene, 2-chloronitrobenzene and p-nitroacetophenone), SiO_2-Ag_2O/void@SiO_2 is better. In contrast, the SiO_2-Ag/Ag_2O/void@SiO_2 catalyst exhibits 100% conversion, 100% selectivity, and 99% yield. When the ratio of H_2O in reaction medium is further increased (Table S1), the excellent photocatalytic performance still is achieved. Even in pure water medium, the SiO_2-Ag/Ag_2O/void@SiO_2 catalyst still displays as high as >99% of selectivity and >98% of yield towards the reduction of three nitroarenes, while SiO_2-Ag_2O/void@SiO_2 produces only 87% conversion and selectivity of 2-chloronitrobenzene, SiO_2-Ag/void@SiO_2 manifests much lower conversion and selectivity of p-nitroacetophenone. In addition, the conversion of nitrobenzene over SiO_2-Ag/Ag_2O/void@SiO_2 catalyst has a turnover frequency (TOF) with 134.7 h^{-1} according to the equation of TOF reported in previous work [15]. This TOF value is

the highest among three photocatalysts (123.0 and 66.5 h^{-1} for SiO_2-Ag_2O/void@SiO_2 and SiO_2-Ag/void@SiO_2, respectively).

The effects of pH and common ions on the photocatalytic performance of the SiO_2-Ag/Ag_2O/void@SiO_2 catalyst were further investigated towards the hydrogenation of nitrobenzene, as shown in Figure S5. Although pH can affect the charge of SiO_2 support because of its surface silanol groups, the electrostatic interaction does not affect the molecular diffusion of catalyst substrates due to electric neutrality of nitroarenes (*e.g.*, NB, 2-NCB and PNAP). When the hydrogenation of NB was carried out in acidic medium (*e.g.,* pH=3 or 5), the pH values of reaction solution exhibit little effect on the photocatalytic performance due to enough amount of hydrogen ions. When basic reaction medium (*e.g.,* pH=8 or 10) was used, a sharply decreased property was observed because the atomic hydrogen was very hard to be produced under visible light irradiation. On the other hand, the common ions (Cl^-, NO_3^-, PO_4^{3-} and SO_4^{2-}) also exhibit significant impact on the photocatalytic performance because they are effective radical scavenger [38].

To confirm the stoichiometry of this photocatalytic hydrogenation [39], we investigated the yields on the hydrogenation of nitrobenzene at different initial concentrations by HPLC. The aniline is obtained almost quantitatively towards the hydrogenation of nitrobenzene in pure water at room temperature (Figure S6), which is in good agreement with the standard curve of amine.

3.4 Role of Ag/Ag_2O and kinetic profiles for the hydrogenation of nitroarenes

When the initial concentration of nitrobenzene increases, SiO_2-Ag/void@SiO_2 photocatalyst produces a obvious decrease in conversion and selectivity in both organic and aqueous media (**Table** S2). Similarly, SiO_2-Ag_2O/void@SiO_2 photocatalyst also exhibits a slow decrease. On the contrary, the

SiO_2-Ag/Ag_2O/void@SiO_2 catalyst still keeps very high yield and selectivity. All these results indicate that the formation of Ag/Ag_2O structure plays a critical role in achieving extremely high activity and selectivity towards the hydrogenation of nitroarenes.

To ascertain the role of Ag and/or Ag_2O as a main photocatalyst under visible-light irradiation, the control experiments were carried out in the dark under identical conditions. Figure S7 shows that the concervion of nitrobenzene is as low as 8.5% without light irradiation at 15°C, even at high reaction temperature (35 °C), the conversion of NB slightly increases to 38.4%. Especially, poor selectivity is observed in the large temperature span (15~35 °C), strongly confirming that excellent activity and selectivity are ascribed to photocatalysis rather than thermal reaction over Ag nanoparticles. On the other hand, the hydrogenation of nitrobenzene was investigated under single-wavelength (λ=400,450,550 nm) irradiation. The experimental results indicate that the high conversion (87.5~98.4%), selectivity (74.2~91.2%), and yield (63.6%-87.9%) of nitrobenzene still are obtained as shown in Figure S8, indicating that Ag_2O works as a main photocatalyst under light irradiation.

The hydrogenation of nitrobenzene was further performed at various temperatures for different time to investigate the effect of temperature on the apparent rate constant (k_{app}) according to the following equation (1) [31]:

$$\ln(C/C_0) = - k_{app}\, t \qquad (1)$$

where C_0 and C are the reactant and initial concentrations of nitrobenzene, respectively. Figure 2a and c show that the k_{app} increases with the increase in temperature, indicating that nitrobenzene molecule does not have so much diffusional limitation to access the photogenerated atomic hydrogen. Based on the Arrhenius equation (2):

$$\ln k_{app} = \ln A - E_a/RT \quad (2)$$

Here, E_a is the energy of activation, A is the pre-exponentialfactor, and R is the general gas constant (8.314 J K^{-1} mol^{-1}). The plot of ln k_{app} versus $1/T$ can be derived as shown in Figure 2b and d. The result shows that E_a for the hydrogneation of nitrobenzene over SiO_2-Ag/Ag_2O/void@SiO_2 photocatalyst is as high as 708.5 kJ/mol, far beyond the value (429.9 kJ/mol) of E_a over SiO_2/void@SiO_2-Ag/Ag_2O catalyst.

3.5 Effect of confinement nanospace on photocatalytic reduction of nitroarenes

To demonstrate the importance of the confined environment in realizing highly efficient selectivity, another two controls, SiO_2/void@SiO_2-Ag/Ag_2O (unconfined bare Ag/Ag_2O, Figure S9a) and SiO_2-Ag/Ag_2O@SiO_2 (without confined nanospace, Figure.S9b), were designed and synthesized under the same condition for further comparison. Table 2 compares their catalytic properties towards the hydrogenation of three nitroarenes under visible-light irradiation. In an organic medium, the SiO_2/void@SiO_2-Ag/Ag_2O demonstrates the lowest yield and selectivity (69~79%) towards three nitroarenes, the introduction of confinement effect can clearly improve the conversion and selectivity of nitroarenes (89~97% for SiO_2-Ag/Ag_2O@SiO_2). In contrast, the confined nanospace causes 100% conversion and selectivity of nitroarenes. In pure aqueous medium, a clear decrease in the conversion and selectivity over two control photocatalysts is observed, while high yield and selectivity (>99%) over the SiO_2-Ag/Ag_2O/void@SiO_2 catalyst are still achieved, indicating that the confined nanospace of photocatalyst may avoid to use organic solvents (*e.g.*, alcohols [3,23,40], THF [35,36,41], and *n*-dodecane [42]) that are widely used during the hydrogenation of nitroarenes.

The highly efficient conversion and selectivity of SiO_2-Ag/Ag_2O/void@SiO_2 photocatalyst are further investigated by evaluating the effect of the initial

concentration on the hydrogenation of nitroarenes. As the initial concentration of nitrobenzene increases, evident decreases in conversion and selectivity over SiO_2/void@SiO_2-Ag/Ag_2O and SiO_2-Ag/Ag_2O@SiO_2 photocatalysts are seen in both organic and aqueous media (Table S3), while the selectivity of nitrobenzene over SiO_2-Ag/Ag_2O/void@SiO_2 photocatalyst almost remains unchanged even when the initial concentration is tripled, suggesting that confined nanospace plays another critical role in obtaining the highly efficient conversion and selectivity.

In addition, our photocatalyst also displays even higher conversion and selectivity (100% and 99.78% in organic and pure water media, respectively) than typical Pd/Si photocatalyst (94% and 83%, respectively) (Table S4). Increasing initial concentration obviously decreased the selectivity of nitrobenzene over the Pd/Si photocatalyst [17], while the nanospace confined photocatalyst still produces as high as 100, 99.32, 99.43 and 97.31% of conversion and selectivity when the initial concentration is doubled, tripled, quintupled, even five-folded, respectively. These results indicate that hydrogenation efficiency of nitrobenzene by our photocatalyst is five times faster than that by typical Pd/Si catalyst [17], no matter whether organic solvent or pure water is used as reactive medium. All these results suggest that the confined nanospace can considerably depress the escape of photo-generated atomic hydrogen and improve the contact probability of atomic hydrogen and nitroarenes, efficiently overcoming the requirement of organic media or harsh reaction conditions that are necessary for almost all the previously reported photocatalysts towards the hydrogenation of nitroarenes (Table S5).

3.6 Recyclability of SiO_2-Ag/Ag_2O/void@SiO_2 photocatalyst

To investigate the reusability and stability of the as-synthesized SiO_2-Ag/Ag_2O/void@SiO_2 photocatalyst, a series of recycling experiments for the

hydrogenation of nitrobenzene were performed under visible-light irradiation through the observation of similar conversion and selectivity for four consecutive recycling [43,44]. The photocatalyst can be easily recovered from each reaction run by centrifugal separation, and then reused for the next run. In the first test, the conversion of nitrobenzene by the fresh solid catalyst is about 100 % within 180 min (Figure S10). The second run also produces 100% conversion and selectivity. Even after four runs, the conversion and selectivity of nitrobenzene are still as high as 97.57%. In particular, the crystalline morphology of Ag/Ag_2O remains very well (Figure S11) and the leaching of Ag does not happen by ICP-OES measurement after four recycle tests, indicating the good chemical stability because of confinement effect (Figure S11).

3.7 Synergistic effect of Ag/Ag_2O and confined nanospace on hydrogenation of nitroarenes

Based on the above results, both the Ag/Ag_2O structure and the confined nanospace effect are playing crucial roles in achieving the extremely high activity and selectivity towards the hydrogenation of nitroarenes under visible-light irradiation. If the Ag/Ag_2O structure was replaced with Ag or Ag_2O nanoparticles, the rapid recombination rate of photo-generated charge pair would take place [33], leading to low photocatalytic efficiency (Tables 1 and S2). The UV–vis absorbance and corresponding Kubelka–Munk plots of three photocatalysts also evidence that the Ag/Ag_2O structure holds the strongest visible-light absorption compared to Ag or Ag_2O confined photocatalysts (Figure S12a, b).

In addition, from the transient photocurrent response and electrical impedance spectroscopy (EIS) Nyquist plots (Figure S12 c, d), the as-synthesized catalyst has the strongest photocurrent intensity in comparison to SiO_2-Ag/Ag_2O@SiO_2 and SiO_2/void@SiO_2-Ag/Ag_2O, indicating the highest transfer efficiency of

photogenerated charge for our photocatalyst due to its high kinetic rate performed in the confined nanospace of double-shelled hollow architecture, which can be further confirmed by the smallest semicircle in the Nyquist plots among the three photocatalysts (Figure S12d).

3.8 molecular dynamics (MD) simulation

To further investigate the effect of nanospace confinement on the hydrogen transfer, we performed molecular dynamics (MD) simulation to build a model system for typical nitrobenzene and hydronium in a confined nanospace and unconfined space behavior in two reactive media, as shown in Movies S1-4. Our simulations clearly demonstrate that the average distance of nitrobenzene and hydronium in a lamellar confinement and unconfined SiO_2 layers are 1.12 and 1.94 nm in organic medium, respectively. This means that in the lamellar confinement environment, nitrobenzene and hydronium have more chances to contact each other with minimum of 0.23 nm (Figure 3 and Figure S13a), suggesting nitrobenzene molecule can form close collision with hydronium, leading to efficient hydrogenation of nitrobenzene. Even in pure water system, the confined nanospace also significantly improves the collision probability of nitrobenzene and hydronium (Figure 3d). The representative structures show that the SiO_2 interface adsorbs hydronium on the surface because of favorable *van der Walls* interaction (Figure S13b), which prevents the nitrobenzene molecule diffusing away from hydronium. The dynamics simulation results indeed confirm that the confined interlayer environment from two-layer SiO_2 plays a critical role in promoting efficient hydrogen transfer from hydrogen donor to nitrobenzene.

3.9 Photocatalytic mechanism towards the hydrogenation of nitroarenes

Based on the experimental results, the theoretical simulation, and the detected intermediates of nitroarenes *via* LC-MS spectra in the presence of the as-synthesized

photocatalyst, we propose a photocatalytic hydrogenation mechanism as shown in Figure 4. Under visible light irradiation at room temperature, Ag_2O is easy to be excited and generates lots of h^+/e^- pairs based on its narrow bandgap (~1.2 eV) [30,45], and the photoinduced electrons in the conduction band of Ag_2O will move to the metallic Ag due to its electron trapping effect [42], while the holes will been consumed in the valence band of Ag_2O by degrading $HCOO^-$ [46], effectively improving electron–hole separation due to its self-stability [30,45]. During hydrogenation of nitroarenes, the electron is received by a proton to produce atomic hydrogen on the metallic silver [17], meanwhile the atomic hydrogen is transfered to nitroarenes, stepwisely forming nitrosobenzene, hydroxylamine and corresponding aniline, while the oxidation of the formate species happens by holes [17].

Thanks to the existence of confined nanospace in the as-synthesized SiO_2-Ag/Ag_2O/void@SiO_2 photocatalyst, the atomic hydrogen can be rapidly utilized to hydrogenate nitroarenes before forming molecular hydrogen because the hydrogenation reaction can occur with the fast reaction kinetics in confined nanospace, leading to a high conversion and selectivity (Figure 5a). In the absence of confined nanospace (SiO_2-Ag/Ag_2O@SiO_2), nitroarenes molecules need to take more time in contacting the photoinduced atomic hydrogen *via* two possible pathways: hydrogenation reduction occurs on the surface of catalyst and within pore channels between inner and outer layers of SiO_2, which enhances the probability of molecular hydrogen formation and thus results in relatively lower photocatalytic efficiency (Figure 5b). In the case of unconfined bare Ag/Ag_2O (SiO_2/void@SiO_2-Ag/Ag_2O), the atomic hydrogen is easy to be escaped from metallic Ag particles, leading to much lower catalytic efficiency for the hydrogenation of nitroarenes (Figure 5c).

4. Conclusion

In summary, we have demonstrated the first confined visible-light-driven photocatalyst with Ag/Ag_2O nanoparticles confined in double-shelled hollow silica spheres. The as-synthesized photocatalyst can significantly promote the hydrogen transfer by enhancing the collision probability between nitroarenes and hydronium because of the confined nanospace effect. Accordingly, this novel photocatalyst displays considerably higher conversion and selectivity than all of the previously reported photocatalysts and commercially available ones. Even in pure water medium, it still presents ultrahigh visible-light catalytic hydrogenation efficiency, and thus can avoid to use organic solvents to drive diffusion and hydrogen-transfer process. The design concept of this new photocatalyst we present here provides a new insight in exploring highly efficient visible-light driven catalysts for the development of eco-friendly organic reactions through the combination of metal/semiconductors and confinement effect.

Conflicts of interest

There are no conflicts to declare.

Acknowledgements

We appreciate the financial support provided for this research by the National Key Research and Development Program of China (2017YFA0204600) and the National Natural Science Foundation of China (21876069, 51721002 and 51673045)

Appendix A. Supplementary data

Supplementary material related to this article can be found, in the online version, at doi: https://doi.org/10.1016/j.cej.

References

[1] L. Wang, E. Guan, J. Zhang, J. Yang, Y. Zhu, Y. Han, M. Yang, C. Cen, G. Fu, B. C. Gates, F. Xiao, Single-site catalyst promoters accelerate metalcatalyzed nitroarene hydrogenation. Nat. Commun 9 (2018) 1362;

[2] J. Camacho-Bunquin, M. Ferrandon, H. Sohn, D. Yang, C. Liu, P. A. Ignacio-de Leon, F. A. Perras, M. Pruski, P. C. Stair, M. Delferro. Chemoselective Hydrogenation with Supported Organoplatinum (IV) Catalyst on Zn(II)-Modified Silica. J. Am. Chem. Soc 140 (2018) 3940−3951;

[3] Y. Dai, C. Li, Y. Shen, S. Zhu, M. S. Hvid, L. Wu, J. Skibsted, Y. Li, J. W. H. Niemantsverdriet, F. Besenbacher, N. Lock, R. Su. Efficient Solar-Driven Hydrogen Transfer by Bismuth-Based Photocatalyst with Engineered Basic Sites. J. Am. Chem. Soc 140 (2018) 16711−16719

[4] L. Zhao, J. Wei, J. Zhang, C. He, C. Duan. Encapsulation of a Quinhydrone Cofactor in the Inner Pocket of Cobalt Triangular Prisms: Combined Light-Driven Reduction of Protons and Hydrogenation of Nitrobenzene. Angew. Chem. Int. Ed 56 (2017) 15284-15288;

[5] B. Mondal, P. S. Mukherjee. Cage Encapsulated Gold Nanoparticles as Heterogeneous Photocatalyst for Facile and Selective Reduction of Nitroarenes to Azo Compounds. J. Am. Chem. Soc 140 (2018) 12592−12601

[6] S. Zhang, C. Chang, Z. Q. Huang, J. Li, Z. Wu, Y. Ma, Z. Zhang, Y. Wang, Y. Qu. High Catalytic Activity and Chemoselectivity of Sub-nanometric Pd Clusters on Porous Nanorods of CeO_2 for Hydrogenation of Nitroarenes. J. Am. Chem. Soc 138 (2016) 2629−2637

[7] R. V. Jagadeesh, K. Murugesan, A. S. Alshammari, H. Neumann, M. Pohl, J. Radnik, M. Beller. MOF-derived cobalt nanoparticles catalyze a general synthesis of amines. Science 358 (2017) 326–332

[8] Y. Peng, Z. Geng, S. Zhao, L. Wang, H. Li, X. Wang, X. Zheng, J. Zhu, Z. Li, R. Si, J. Zeng. Pt Single Atoms Embedded in the Surface of Ni Nanocrystals as Highly Active Catalysts for Selective Hydrogenation of Nitro Compounds. Nano Lett 18 (2018) 3785−3791;

[9] B. Zhang, H. Asakura, J. Zhang, J. Zhang, S. De, N. Yan. Stabilizing a Platinum1 Single-Atom Catalyst on Supported Phosphomolybdic Acid without Compromising Hydrogenation Activity. Angew. Chem. Int. Ed 55 (2016) 8319-8323;

[10] P. Ryabchuk, G. Agostini, M. Pohl, H. Lund, A. Agapova, H. Junge, K. Junge, M. Beller. Intermetallic nickel silicide nanocatalyst—A non-noble metal–based general hydrogenation catalyst. Sci. Adv 4 (2018) eaat0761

[11] P. Zhou, L. Jiang, F. Wang, K. Deng, K. Lv, Z. Zhang. High performance of a cobalt–nitrogen complex for the reduction and reductive coupling of nitro compounds into amines and their derivatives. Sci. Adv 3 (2017) e1601945;

[12] R. V Jagadeesh, T. Stemmler, A. Surkus, H. Junge, K. Junge, M. Beller. Hydrogenation using iron oxide–based nanocatalysts for the synthesis of amines. Nat. Protocols 10 (2015) 548-557;

[13] T. Ye, Y. Lu, J. Li, T. Nakao, H. Yang, T. Tada, M. Kitano, H. Hosono. Copper-Based Intermetallic Electride Catalyst for Chemoselective Hydrogenation Reaction. J. Am. Chem. Soc 139 (2017) 17089-17097

[14] Q. Xiao, S. Sarina, E. R. Waclawik, J. Jia, J. Chang, J. D. Riches, H. Wu, Z. Zheng, H. Zhu. Alloying Gold with Copper Makes for a Highly Selective Visible-Light Photocatalyst for the Reduction of Nitroaromatics to Anilines. ACS Catal 6 (2016) 1744−175

[15] C. Hao, X. Guo, Y. Pan, S. Chen, Z. Jiao, H. Yang, X. Guo. Visible-Light-Driven Selective Photocatalytic Hydrogenation of Cinnamaldehyde over Au/SiC Catalysts. J. Am. Chem. Soc 138 (2016) 9361−9364;

[16] J. Song, Z. Huang, L. Pan, K. Li, X. Zhang, L. Wang, J. Zou. Review on selective hydrogenation of nitroarene by catalytic, photocatalytic and electrocatalytic reactions. Appl. Catal. B: Environ 227 (2018) 386–408

[17] K. Tsutsumi, F. Uchikawa, K. Sakai, K. Tabata. Photoinduced Reduction of Nitroarenes Using a Transition-Metal-Loaded Silicon Semiconductor under Visible Light Irradiation. ACS Catal 6 (2016) 4394−4398

[18] P. Sharma, Y. Sasson. Sustainable visible light assisted in situ hydrogenation via a magnesium–water system catalyzed by a Pd-g-C_3N_4 photocatalyst. Green Chem 21 (2019) 261–268

[19] Q. Xiao, Z. Liu, A. Bo, S. Zavahir, S. Sarina, S. Bottle, J. D. Riches, H. Zhu. Catalytic Transformation of Aliphatic Alcohols to Corresponding Esters in O_2 under Neutral Conditions Using Visible-Light Irradiation. J. Am. Chem. Soc 137 (2015) 1956−1966

[20] P. Ji, K. Manna, Z. Lin, X. Feng, A. Urban, Y. Song, W. Lin. Single-Site Cobalt Catalysts at New $Zr_{12}(\mu_3\text{-}O)_8(\mu_3\text{-}OH)_8(\mu_2\text{-}OH)_6$Metal–Organic Framework Nodes for Highly Active Hydrogenation of Nitroarenes, Nitriles, and Isocyanides. J. Am. Chem. Soc 139 (2017) 7004-7011;

[21] Y. Tan, X. Liu, L. Zhang, A. Wang, L. Li, X. Pan, S. Miao, M. Haruta, H. Wei, H. Wang, F. Wang, X. Wang, T. Zhang. ZnAl‐Hydrotalcite‐Supported Au_{25} Nanoclusters as Precatalysts for Chemoselective Hydrogenation of 3‐Nitrostyrene. Angew. Chem. Int. Ed 56 (2017) 2709-2713;

[22] L. Zhao, J. Wei, J. Lu, C. He, C. Duan. Renewable Molecular Flasks with NADH Models: Combination of Light‐Driven Proton Reduction and Biomimetic Hydrogenation of Benzoxazinones. Angew. Chem. Int. Ed 56 (2017) 8692-8696;

[23] Y. Song, H. Wang, Z. Wang, B. Guo, K. Jing, Y. Li, L. Wu. Selective Photocatalytic Synthesis of Haloanilines from Halonitrobenzenes over Multifunctional AuPt/Monolayer Titanate Nanosheet. ACS Catal 8 (2018) 9656−9664;

[24] M. Fan, W. D. Wang, Y. Zhu, X. Sun, F. Zhang, Z. Dong. Palladium clusters confined in triazinyl-functionalized COFs with enhanced catalytic activity. Appl. Catal, B: Environ 257 (2019) 117942

[25] Q. Zhang, X. Jin, Z. Xu, J. Zhang, U. F. Rendon, L. Razzari, M. Chaker, D. Ma. Plasmonic Au-Loaded Hierarchical Hollow Porous TiO_2 Spheres: Synergistic Catalysts for Nitroaromatic Reduction. J. Phys. Chem. Lett 9 (2018) 5317-5326

[26] G. Xiao, P. Li, Y. Zhao, S. Xu, H. Su. Visible‐Light‐Driven Chemoselective Hydrogenation of Nitroarenes to Anilines in Water through Graphitic Carbon Nitride Metal‐Free Photocatalysis. Chem. Asian J 13 (2018) 1950-1955

[27] M. Chen, L. Wu, S. Zhou, B. You, A method for the fabrication of monodisperse hollow silica spheres. Adv. Mater 18 (2006) 801-806

[28] Y. Zhang, Y. Zhao, S. Cao, Z. Yin, L. Cheng, L. Wu. Design and Synthesis of Hierarchical SiO_2@C/TiO_2 Hollow Spheres for High-Performance Supercapacitors. ACS Appl. Mater. Interfaces 9 (2017) 29982−29991

[29] C. Jiang, K. Hara, A. Fukuoka. Low‐Temperature Oxidation of Ethylene over Platinum Nanoparticles Supported on Mesoporous Silica. Angew. Chem. Int. Ed 52 (2013) 6265-6268

[30] Y. Cui, Q. Ma, X. Deng, Q. Meng, X. Cheng, M. Xie, X. Li, Q. Cheng, H. Liu. Fabrication of Ag-Ag_2O/reduced TiO_2 nanophotocatalyst and its enhanced visible light driven photocatalytic performance for degradation of diclofenac solution. Appl. Catal, B: Environ 206 (2017) 136–145

[31] S. Cao, J. Chang, L. Fang, L. Wu. Metal Nanoparticles Confined in the Nanospace of Double-Shelled Hollow Silica Spheres for Highly Efficient and Selective Catalysis. Chem. Mater 28 (2016) 5596−5600

[32] X. Han, X. He, L. Sun, X. Han, W. Zhan, J. Xu, X. Wang, J. Chen. Increasing Effective Photogenerated Carriers by Insitu Anchoring Cu_2O Nanoparticles on Nitrogen-doped Porous Carbon Yolk-shell Cuboctahedral Framework. ACS Catal. 8 (2018) 3348-3356.

[33] J. Chen, H. Che, K. Huang, C. Liu, W. Shi. Fabrication of a ternary plasmonic photocatalyst CQDs/Ag/Ag_2O to harness charge flow for photocatalytic elimination of pollutants. Appl. Catal, B: Environ 192 (2016) 134–144

[34] S. Zhao, J. Chen, Y. Liu, Y. Jiang, C. Jiang, Z. Yin, Y. Xiao, S. Cao. Silver Nanoparticles Confined in Shell-in-Shell Hollow TiO_2 Manifesting Efficiently Photocatalytic Activity and Stability. Chem. Eng. J 367 (2019) 249-259

[35] R. V. Jagadeesh, A. Surkus, H. Junge, M. Pohl, J. Radnik, J. Rabeah, H. Huan,V. Schünemann, A. Brückner, M. Beller. Nanoscale Fe_2O_3-based catalysts for selective hydrogenation of nitroarenes to anilines. Science 342 (2013) 1073-1076;

[36] J. Zhang, L. Wang, Y. Shao, Y. Wang, B. C. Gates, F. Xiao. A Pd@Zeolite Catalyst for Nitroarene Hydrogenation with High Product Selectivity by Sterically Controlled Adsorption in the Zeolite Micropores. Angew. Chem. Int. Ed 56 (2017) 9747-9751

[37] Y. Duan, T. Song, X. Dong, Y. Yang. Enhanced catalytic performance of cobalt nanoparticles coated with a N, P-co-doped carbon shell derived from biomass for transfer hydrogenation of functionalized nitroarenes. Green Chem 20 (2018) 2821-2828

[38] D. Huang, J. Lia, G. Zeng, W. Xue, S. Chen, Z. Li, R. Deng, Y. Yang, M. Cheng. Facile construction of hierarchical flower-like Z-scheme $AgBr/Bi_2WO_6$ photocatalysts for effective removal of tetracycline: Degradation pathways and mechanism. Chem. Eng. J. 375 (2019) 121991

[39] M. Fukui, W. Koshida, A. Tanaka, K. Hashimoto, H. Kominami. Photocatalytic hydrogenation of nitrobenzenes to anilines over noble metal-free TiO_2 utilizing methylamine as a hydrogen donor. Appl. Catal B: Environ, 2019, 118446

[40] Z. Yin, Y. Wang, C. Song, L. Zheng, N. Ma, X. Liu, S. Li, L. Lin, M. Li, Y. Xu, W. Li, G. Hu, Z. Fang, D. Ma. Hybrid Au–Ag Nanostructures for Enhanced Plasmon-Driven Catalytic Selective Hydrogenation through Visible Light Irradiation and Surface-Enhanced Raman Scattering. J. Am. Chem. Soc 140 (2018) 864−867

[41] R. V. Jagadeesh, K. Natte, H. Junge, M. Beller, Nitrogen-Doped Graphene-Activated Iron-Oxide-Based Nanocatalysts for Selective Transfer Hydrogenation of Nitroarenes. ACS Catal 5 (2015) 1526−1529

[42] Q. Zhang, S. Li, M. Zhu, Y. Liu, H. He, Y. Cao. Direct Reductive Amination of Aldehydes with Nitroarenes Using Bio-renewable Formic Acid as a Hydrogen Source. Green Chem 18 (2016) 2507-2513

[43] X. Zhang, Y. Zhao, S. Xu, Y. Yang, J. Liu, Y. Wei, Q. Yang. Polystyrene sulphonic acid resins with enhanced acid strength via macromolecular self-assembly within confined nanospaces. Nat. Commun 5 (2014) 3170;

[44] W. Zhang, G. Lu, C. Cui, Y. Liu, S. Li, W. Yan, C. Xing, Y. R. Chi, Y. Yang, F. Huo. A Family of Metal-Organic Frameworks Exhibiting Size Selective Catalysis with Encapsulated Noble-Metal Nanoparticles. Adv. Mater 26 (2014) 4056–4060

[45] M. Yang, M. Gao, M. Hong, G. W. Ho. Visible-to-NIR Photon Harvesting: Progressive Engineering of Catalysts for Solar-Powered Environmental Purification and Fuel Production. Adv. Mater 30 (2018) 1802894

[46] L. Clarizia, I. D. Somma, R. Marotta, P. Minutolo, R. Villamaina, R. Andreozzi. Photocatalytic reforming of formic acid for hydrogen production in aqueous solutions containing cupric ions and TiO_2 suspended nanoparticles under UV-simulated solar radiation. Appl. Catal A: Gen, 518 (2016) 181-188

Figures and Tables

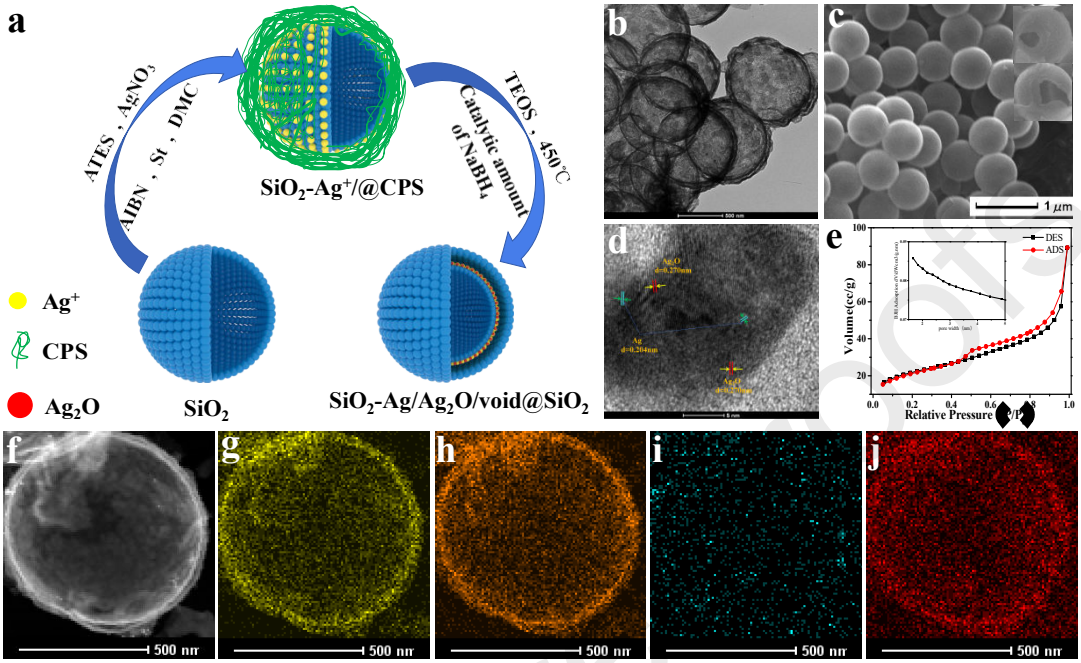

Figure 1. The preparation and characterization of the photocatalyst. (a) Illustration for the synthetic scheme of the SiO_2-Ag/Ag_2O/void@SiO_2 photocatalyst. (b) TEM image. (c) SEM image. (d) HRTEM image, inset, the artificially broken spheres. (e) BET. (f) STEM images and EDX mapping (g: Si, h: O, i: Ag, and j: C).

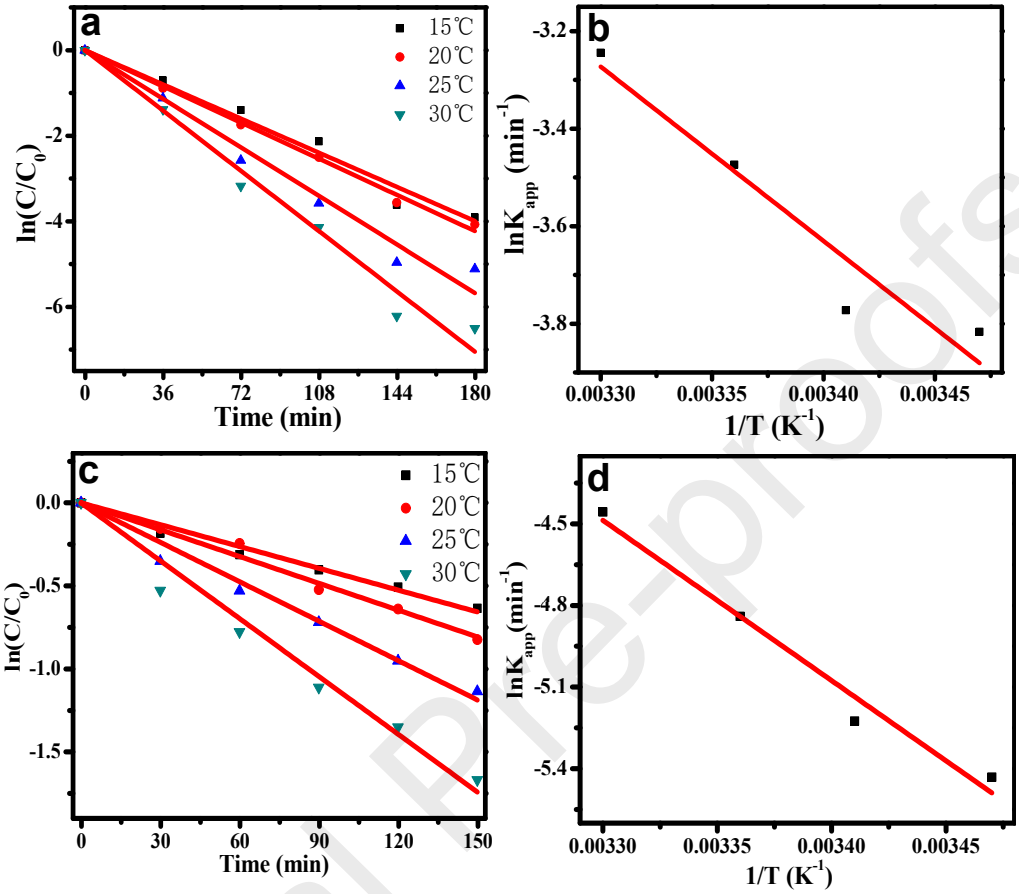

Figure 2 Plot of ln(C/C$_0$) versus t (min) and Arrhenius plot of ln k_{app} versus 1/T (K−1) for catalytic reduction of NB in the presence of SiO_2/void@SiO_2-Ag/Ag_2O (a,b) or SiO_2-Ag/Ag_2O/void@SiO_2 (c,d) photocatalyst in aqueous medium.

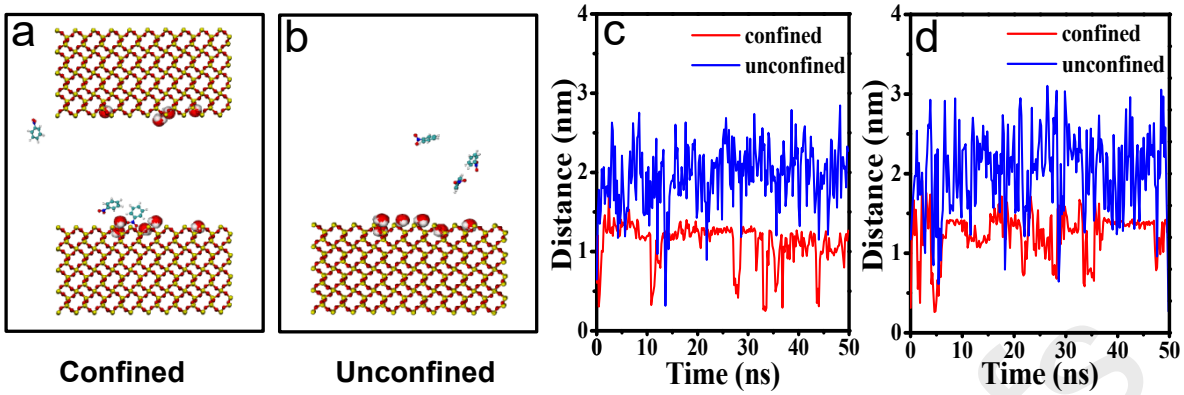

Figure 3 the molecular dynamics simulation. The structure of representative model system: the distance between nitrobenzene and hydronium in the confined interlayer environment between two SiO_2 layers (**a**) and in the unconfined surface of outer SiO_2 layer (**b**); (**c**) the minimum distance between nitrobenzene and hydronium in organic medium; (**d**) the minimum distance between nitrobenzene and hydronium in pure water.

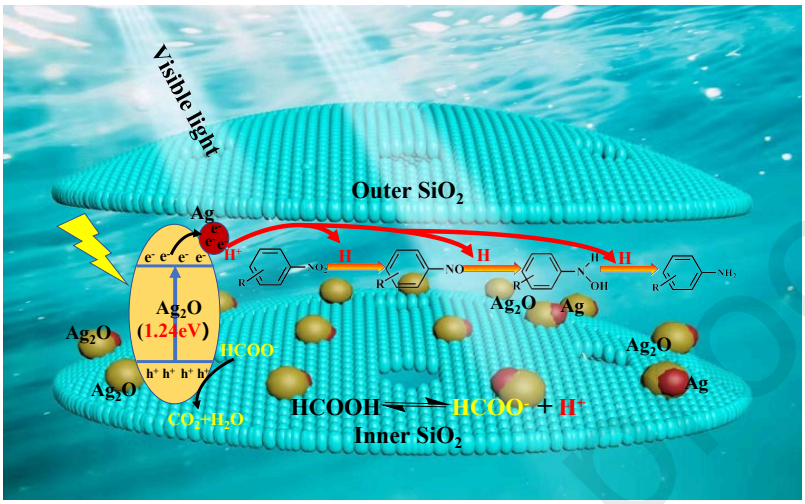

Figure 4. Photocatalytic mechanism of hydrogenation of nitroarenes

Table 1 Hydrogenation of nitroarenes to produce aniline under visible-light irradiation

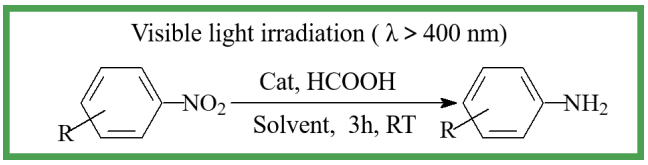

Catalyst	Solvent	NB			2-NCB			PNAP		
		Conv. (%)	Select. (%)	Yield (%)	Conv. (%)	Select. (%)	Yield (%)	Conv. (%)	Select. (%)	Yield (%)
SiO_2-Ag/Ag_2O/void@SiO_2	2-propanol /H_2O	100	100	99.0	100	100	99.0	100	100	99.0
SiO_2-Ag_2O/void@SiO_2		99.75	99.75	97.51	98.20	98.20	94.50	97.84	97.84	93.81
SiO_2-Ag/void@-SiO_2		79.73	79.73	62.30	59.42	59.42	34.61	65.13	65.13	41.57
SiO_2-Ag/Ag_2O/void@SiO_2	H_2O	99.78	99.78	98.57	99.75	99.75	98.51	99.40	99.40	98.13
SiO_2-Ag_2O/void@SiO_2		95.48	95.48	89.34	87.00	87.00	74.18	89.17	89.17	77.92
SiO_2-Ag/void@-SiO_2		64.99	64.99	41.39	34.68	34.68	11.79	20.85	20.85	4.26

Reaction conditions: nitroarenes (0.05 mmol), formic acid (8.3 mg), photocatalyst (25 mg), water (1.1 mL)/2-propanol (9.1 mL) or water (10.2 mL) medium, visible-light irradiation (xenon lamp, 300 W) with an UV cutoff filter (λ>400 nm), Time=3 h, Room temperature (RT).

Table 2 the effect of confined nanospace on the hydrogenation of nitroarenes

Catalyst	Solvent	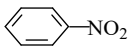 NB			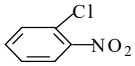 2-NCB			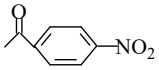 PNAP		
		Conv. (%)	Select. (%)	Yield (%)	Conv. (%)	Select. (%)	Yield (%)	Conv. (%)	Select. (%)	Yield (%)
SiO_2-Ag/Ag_2O/void@SiO_2 (with confined nanospace)	2-propanol /H_2O	100	100	99.0	100	100	99.0	100	100	99.0
SiO_2-Ag/Ag_2O@SiO_2 (without confined nanospace)		97.64	97.64	93.43	96.63	96.63	91.51	89.37	89.37	78.27
SiO_2/void@SiO_2-Ag/Ag_2O (unconfined bare-Ag/Ag_2O)		74.56	74.56	54.48	79.30	79.30	61.63	69.78	69.78	47.72
SiO_2-Ag/Ag_2O/void@SiO_2 (with confined nanospace)	H_2O	99.78	99.78	98.57	99.75	99.75	98.51	99.40	99.40	98.13
SiO_2-Ag/Ag_2O@SiO_2 (without confined nanospace)		95.32	95.32	89.04	87.05	87.05	74.26	85.59	85.59	71.79
SiO_2/void@SiO_2-Ag/Ag_2O (unconfined bare-Ag/Ag_2O)		70.71	70.71	49.0	55.70	55.70	30.40	64.14	64.14	40.32

Reaction conditions: nitroarenes (0.05 mmol), formic acid (8.3 mg), photocatalyst (25 mg), water (1.1 mL)/2-propanol (9.1 mL) or water (10.2 mL) medium, visible-light irradiation (xenon lamp,300 W) with an UV cut-off filter (λ>400 nm), Time=3 h, Room temperature.

Graphical abstract

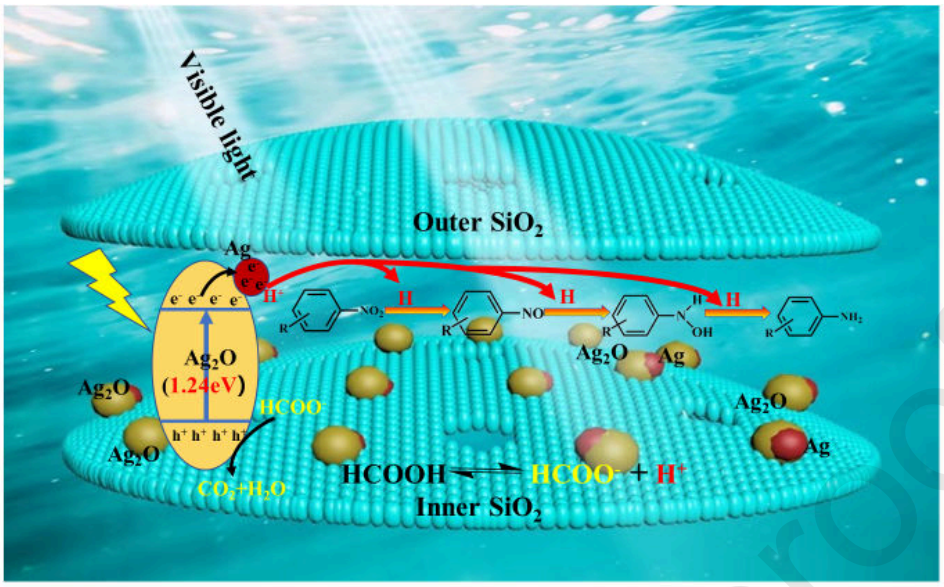

- The first example of the confined visible-light driven catalyst was reported.
- Ag/Ag_2O confined in the nanospace of double-shelled hollow silica were successfully synthesized.
- The as-synthesized photocatalyst exhibited superior activity, selectivity, and recyclability than other catalysts.
- Molecular dynamics simulation was used to build a model system for the hydrogenation of nitroarenes.